Large Intragenic Deletion in *DSTYK* Underlies Autosomal-Recessive Complicated Spastic Paraparesis, SPG23

John Y.W. Lee,[1] Chao-Kai Hsu,[2,3,25] Magdalene Michael,[4,25] Arti Nanda,[5,25] Lu Liu,[6] James R. McMillan,[6] Celine Pourreyron,[7] Takuya Takeichi,[1,8] Jakub Tolar,[9,10] Evan Reid,[11,12] Thomas Hayday,[4] Sergiu C. Blumen,[13,14] Saif Abu-Mouch,[15] Rachel Straussberg,[16,17] Lina Basel-Vanagaite,[17,18,19,20] Yael Barhum,[21,22] Yasmin Zouabi,[16] Hejab Al-Ajmi,[5] Hsin-Yu Huang,[2] Ting-Chien Lin,[2] Masashi Akiyama,[8] Julia Y.Y. Lee,[2] W.H. Irwin McLean,[23] Michael A. Simpson,[24] Maddy Parsons,[4] and John A. McGrath[1,23,*]

SPG23 is an autosomal-recessive neurodegenerative subtype of lower limb spastic paraparesis with additional diffuse skin and hair dyspigmentation at birth followed by further patchy pigment loss during childhood. Previously, genome-wide linkage in an Arab-Israeli pedigree mapped the gene to an approximately 25 cM locus on chromosome 1q24–q32. By using whole-exome sequencing in a further Palestinian-Jordanian SPG23 pedigree, we identified a complex homozygous 4-kb deletion/20-bp insertion in *DSTYK* (dual serine-threonine and tyrosine protein kinase) in all four affected family members. *DSTYK* is located within the established linkage region and we also found the same mutation in the previously reported pedigree and another Israeli pedigree (total of ten affected individuals from three different families). The mutation removes the last two exons and part of the 3′ UTR of *DSTYK*. Skin biopsies revealed reduced DSTYK protein levels along with focal loss of melanocytes. Ultrastructurally, swollen mitochondria and cytoplasmic vacuoles were also noted in remaining melanocytes and some keratinocytes and fibroblasts. Cultured keratinocytes and fibroblasts from an affected individual, as well as knockdown of *Dstyk* in mouse melanocytes, keratinocytes, and fibroblasts, were associated with increased cell death after ultraviolet irradiation. Keratinocytes from an affected individual showed loss of kinase activity upon stimulation with fibroblast growth factor. Previously, dominant mutations in *DSTYK* were implicated in congenital urological developmental disorders, but our study identifies different phenotypic consequences for a recurrent autosomal-recessive deletion mutation in revealing the genetic basis of SPG23.

The hereditary spastic paraplegias (HSPs) are a group of inherited disorders characterized by spastic paralysis of the lower limbs. The genetic basis of HSPs is complex, with more than 70 subtypes.[1] Among these, spastic paraplegia type 23 (SPG23 [MIM: 270750]) is a rare subtype presenting in childhood with progressive spastic paraplegia associated with peripheral neuropathy, skin pigment abnormalities (i.e., vitiligo, hyperpigmentation, diffuse lentigines), and premature graying of hair. To date, only five reports have been documented (Table S1).[2–6] The affected individuals in three of these reports were from the Middle East (two Arab-Israeli and one Jordanian),[2–4] another individual was of North European descent,[5] and the most recent case was from India.[6] In the Arab-Israeli family originally reported in 1985,[4] linkage analysis mapped the causative gene to a 25-cM region on chromosome 1q24–q32 (maximum LOD score of 3.05).[7] This interval contained approximately 276 genes but no candidate gene and pathogenic mutations were identified.

To identify mutations that cause SPG23, we investigated an additional, previously unreported, Kuwaiti-Jordanian family (family 1) containing four affected individuals with evidence of autosomal-recessive inheritance (Figure 1A). The proband, a 22-year-old male Palestinian (individual

[1]St John's Institute of Dermatology, King's College London (Guy's Campus), London SE1 9RT, UK; [2]Department of Dermatology, National Cheng Kung University Hospital, College of Medicine, National Cheng Kung University, Tainan 701, Taiwan; [3]Institute of Clinical Medicine, College of Medicine, National Cheng Kung University, Tainan 701, Taiwan; [4]Randall Division of Cell and Molecular Biophysics, King's College London (Guy's Campus), London SE1 9RT, UK; [5]As'ad Al-Hamad Dermatology Center, Al-Sabah Hospital, Kuwait City 13001, Kuwait; [6]The National Diagnostic EB Laboratory, Viapath, St Thomas' Hospital, London SE1 7EH, UK; [7]Jacqui Wood Cancer Centre, University of Dundee, Ninewells Hospital and Medical School, Dundee DD1 9SY, UK; [8]Department of Dermatology, Nagoya University Graduate School of Medicine, Nagoya 466-8560, Japan; [9]Department of Pediatrics, Division of Blood and Marrow Transplantation, University of Minnesota, Minneapolis, MN 55455, USA; [10]Stem Cell Institute, University of Minnesota, Minneapolis, MN 55455, USA; [11]Cambridge Institute for Medical Research (CIMR), University of Cambridge, Cambridge CB2 0XY, UK; [12]Department of Medical Genetics, Addenbrooke's Hospital, University of Cambridge, Cambridge CB2 0QQ, UK; [13]Department of Neurology, Hillel Yaffe Medical Center, Hadera 38100, Israel; [14]Rappaport Faculty of Medicine, Technion, Israel Institute of Technology, Haifa 3525433, Israel; [15]Liver Unit, Department of Internal Medicine B, Hillel Yaffe Medical Center, Hadera 38100, Israel; [16]Neurogenetic Service, Neurology Institute, Schneider Children's Medical Center, Petah Tikva 49202, Israel; [17]Sackler Faculty of Medicine, Tel Aviv University, Tel Aviv 69978, Israel; [18]Raphael Recanati Genetic Institute, Rabin Medical Center, Beilinson Campus, Petah Tikva 49100, Israel; [19]Pediatric Genetics Unit, Schneider Children's Medical Center, Petah Tikva 49202, Israel; [20]Felsenstein Medical Research Center, Rabin Medical Center, Petah Tikva 4941492, Israel; [21]Laboratory of Clinical Neuroscience, Felsenstein Medical Research Center, Rabin Medical Center, Petah Tikva 4941492, Israel; [22]Department of Neurology, Sackler Faculty of Medicine, Tel Aviv University, Tel Aviv 69978, Israel; [23]Centre for Dermatology and Genetic Medicine, Division of Molecular Medicine, University of Dundee, Dundee DD1 5EH, UK; [24]Department of Medical and Molecular Genetics, King's College London, School of Medicine, Guy's Hospital, London SE1 9RT, UK
[25]These authors contributed equally to this work
*Correspondence: john.mcgrath@kcl.ac.uk
http://dx.doi.org/10.1016/j.ajhg.2017.01.014.

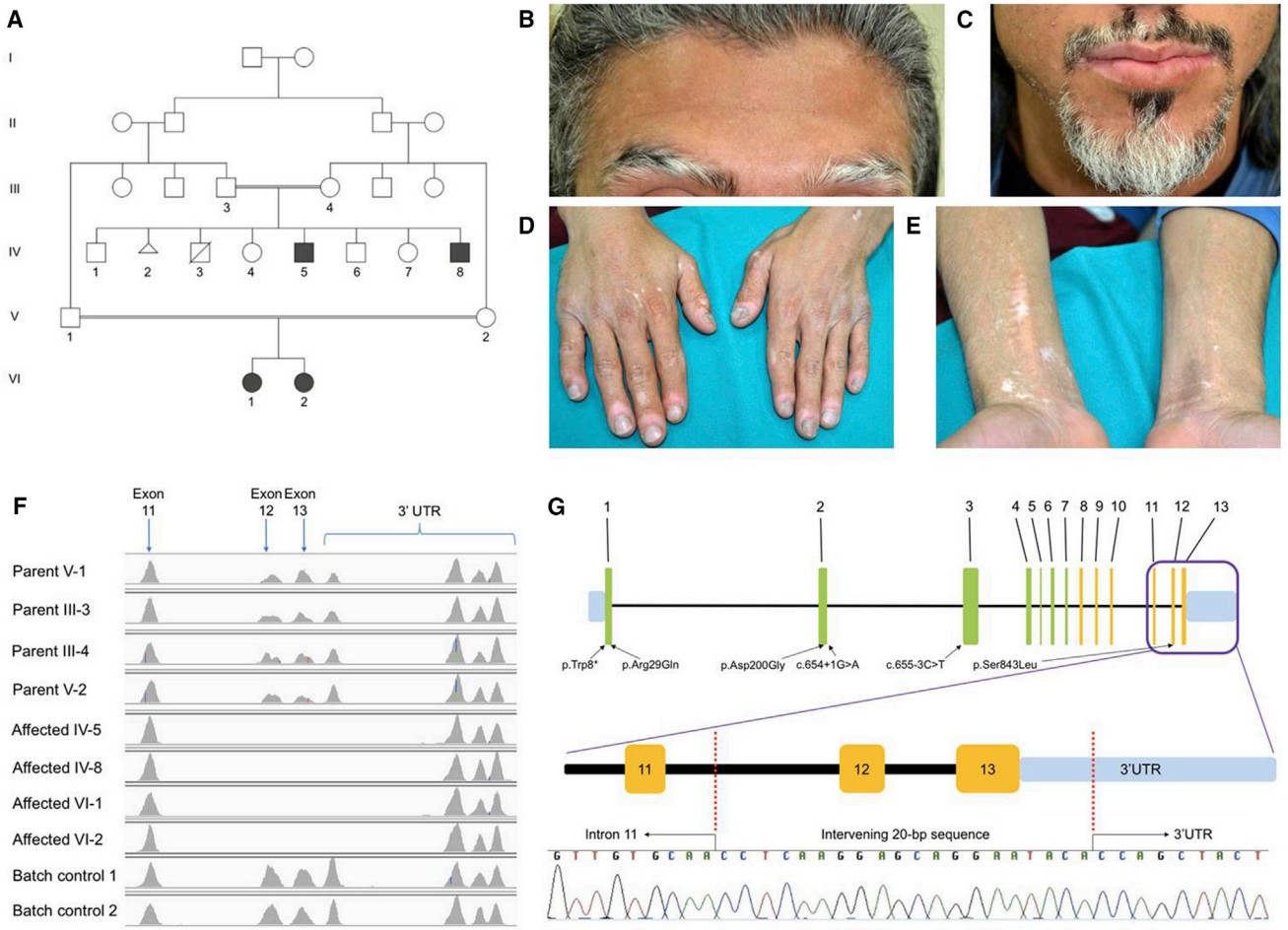

Figure 1. Pedigree and Molecular Pathology of SPG23
(A) The family pedigree of family 1. Squares denote male family members and circles female family members; filled-in symbols indicate clinically affected individuals. The triangle (IV-2) refers to a spontaneous abortion.
(B) Affected individual IV-5 with gray/white hair in the scalp and eyebrows and dyspigmentation on the forehead.
(C) Similar changes affecting hair follicle pigmentation are present in the beard area (individual IV-5).
(D) Blotchy dyspigmentation, hypopigmentation, and depigmentation on the dorsum of the hands with marked pigment loss and some erythema around the finger nails.
(E) Loss of skin pigment (vitiligo-like lesions) on the flexural aspects of the wrists and forearms (individual IV-5).
(F) Integrative Genomics Viewer analysis reveals homozygous loss of exons 12 and 13 and part of the 3′ UTR of *DSTYK* in affected individuals IV-5, IV-8, VI-1, and VI-2. Heterozygous changes are implicated in the parental samples (III-3, III-4, V-1, and V-2).
(G) Schematic of *DSTYK* to show the homozygous mutation and Sanger sequencing confirmation of the 4-kb deletion/20-bp insertion in genomic DNA (affected individual IV-5). The schematic also illustrates the previous mutations in *DSTYK* identified in a different disorder, autosomal-dominant congenital anomalies of the kidney and urinary tract-1 (CAKUT1).

IV-5), presented with life-long silvery-gray hair on the scalp, eyebrows (Figure 1B), and eyelashes; his beard area (Figure 1C) and secondary sexual hair were also affected by focal pigment loss after puberty. In addition, during childhood he had patchy pigmentary changes on his skin, with later onset (early 20s) of more depigmented, vitiligo-like lesions on the lips, hands, and forearms (Figures 1D and 1E). He developed a waddling gait from the age of 2–3 years with subsequent emergence of spastic paraplegia requiring wheelchair use from the age of 9 years. He is of normal intelligence, and there is no history of epilepsy, sensorineural deafness, or other motor or sensory neurologic manifestations. He is the third of six living siblings from a parent-related (first cousin) family, and his younger brother (IV-8) and two female cousins (VI-1 and VI-2) have similar phenotypes. His bladder function is normal but he and his younger brother both experience bowel urgency and incontinence. The younger brother also experienced convulsions at the age of 6 years after a high-grade fever. In the proband (IV-5), laboratory tests (full blood count and serum biochemistry) were all unremarkable. Brain magnetic resonance imaging showed no gross abnormalities. An X-ray of his hips showed bilateral dislocation. Ultrasound of his abdomen and pelvis revealed a horseshoe kidney malformation, although no urogenital anomalies were detected in his affected brother (IV-8); screening has not yet been undertaken in either of the two other affected family members.

To identify the underlying molecular genetic defect in these individuals, we obtained blood for genetic testing and skin samples (ellipse of skin taken under local anesthesia by 1% lignocaine) from members of this family in adherence to the Declaration of Helsinki. Whole-exome sequencing was performed using genomic DNA extracted from peripheral blood from all affected individuals and their respective parents. Whole-exome capture was performed on these eight samples using in-solution hybridization (Agilent All Exon V4) and sequence data were generated on the Illumina HiSeq 2000. The reads produced were aligned to the reference human genome using the NovoAlign software package (Novocraft Technologies Sdn Bhd). Duplicate reads, arising from PCR clonality or optical duplicates, and reads mapping to multiple regions were removed from downstream analysis. A summary of exome coverage data is presented in Table S2.

Whole-exome sequencing failed to reveal any rare, pathogenic homozygous single-nucleotide variants or indels that were present in all four affected individuals. However, we observed two blocks of homozygosity that were shared among all four affected individuals, namely a 9.9-Mb block at chromosome 1q32 and a 4.4-Mb block at chromosome 9p13. Because the SPG23 locus had previously been mapped to chromosome 1q24–q32,[7] we analyzed copy-number variation (CNV) data with the ExomeDepth software package[8] and identified a putative homozygous intragenic deletion in *DSTYK* in each of the affected individuals, which completely removed the last two exons (12 and 13) along with part of the 3′ UTR (Figure 1F). Using a "primer walk" approach, the precise breakpoints of the deletion in intron 11 and the 3′ UTR were identified (Figure 1G), with coordinates from chromosome 1: 205,145,663–205,149,750 (GRCh38/hg38 assembly). This mutation was absent from an in-house exome bank and public databases, including DECIPHER,[9] Database of Genomic Variants,[10] and Copy Number Variation in Disease.[11] Intriguingly, this 4-kb deletion was accompanied by the insertion of an intervening 20-bp sequence. Using the Basic Local Alignment Search Tool (BLAST), this sequence was shown to originate from 5,765 bp downstream of the original stop codon (chr1: 205,141,774–205,141,793) and inverted prior to re-insertion. Additionally, all affected individuals carried the common SNP rs3902193. Complex CNVs similar to the mutation identified here have previously been reported to be associated with human genetic disease.[12,13] We then assessed correlation of the mutation with disease status in the rest of the family by designing two further pairs of allele-specific primers to selectively amplify the wild-type and mutant alleles (Table S3) and confirmed that this deletion in *DSTYK* fully segregates with phenotype (Figure S1).

Next, we investigated whether the previously reported Arab-Israeli pedigree (family 2) linked to 1q24–q32[7] and another unreported Israeli family (family 3) with an SPG23 phenotype also carried a recessive mutation in *DSTYK*. We found that the affected individuals in these two families also carried the same intragenic deletion, and this mutation also segregated with phenotype in the rest of the family (Figures S2 and S3). Because all three pedigrees originated from the Middle East, we explored the possibility that the deletion in *DSTYK* may represent a founder mutation and that these families may be distantly related. Using a number of microsatellite markers around the *DSTYK* locus (Figure S4), we found that the three families had a shared haplotype around the mutation, but with a refined area of linkage of approximately 9.6 cM between D1S413 and D1S2692. *DSTYK* is included within the new interval (along with 202 other genes).

DSTYK, also known as Dusty protein kinase, receptor interacting protein 5 (RIP5), or RIP kinase 5 (RIPK5), encodes dual serine-threonine and tyrosine protein kinase, an enzyme implicated as a regulator of cell death.[14] DSTYK was found to induce both caspase-dependent and caspase-independent cell death in a dose-dependent manner,[14] although subsequent studies have challenged the notion that DSTYK is a RIP5 family member.[15,16] *DSTYK* mRNA is expressed in multiple tissues, although normalized expression distribution is highest in the spinal cord, pineal gland, and skin according to the SOURCE database.[17] With regard to human disease, heterozygous mutations in *DSTYK* were identified as a frequent cause of autosomal-dominant congenital anomalies of the kidney and urinary tract-1 (CAKUT1 [MIM: 610805]).[18] Notably, *DSTYK* mutations were found in 2.3% of CAKUT1-affected case subjects, suggesting that DSTYK is a major determinant of human urinary tract development.[18] Interestingly, among individuals with these autosomal-dominant *DSTYK* mutations, three family members with a splice site mutation had epilepsy and an unrelated individual with a nonsense mutation experienced early-onset ataxia. Nevertheless, no skin or pigmentary changes were associated with these heterozygous mutations.[18]

Next, we assessed DSTYK pathology in skin, after written and informed consent according to a protocol approved by the St Thomas' Hospital Ethics Committee (Molecular basis of inherited skin disease: 07/H0802/104). Peri-lesional skin biopsies were obtained from the leg of affected individual IV-5 of family 1 and assessed by immunofluorescence and transmission electron microscopy (see Table S5 for antibody details). Immunofluorescence microscopy of DSTYK using both N-terminal and C-terminal antibodies showed markedly reduced labeling (Figures 2A and 2B) in the IV-5 skin compared to control subjects. Transmission electron microscopy revealed focal loss of melanocytes with some of the remaining melanocytes showing ultrastructural features of swollen mitochondria and cytoplasmic vacuoles (Figure 2C), but these abnormalities were not present in apparently unaffected melanocytes in the same affected individual (Figure S8). These enlarged mitochondria with abnormal cristae were also observed in other cell types such as fibroblasts and keratinocytes (Figure 2D). These pathological findings indicate an increased susceptibility of mutant cells to stress and cell death.

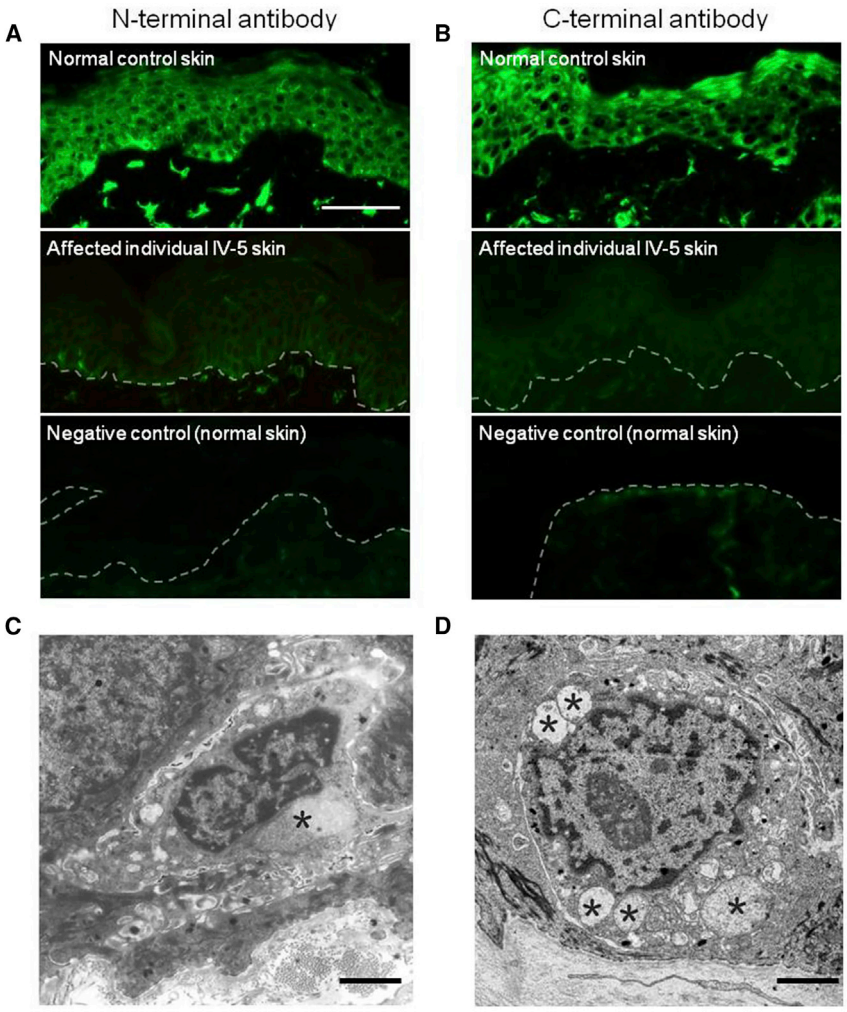

Figure 2. Skin Pathology in SPG23
(A) Immunofluorescence microscopy using a DSTYK N-terminal antibody (NBP1-92336, 1:500, Novus Biologicals) in normal skin (top) reveals bright pan-epidermal cytoplasmic staining with focal accentuation in basal epidermal melanocytes and dermal fibroblasts. In affected individual (IV-5) skin (middle), there is markedly reduced labeling, with an absence of staining in the negative control (bottom) (scale bar represents 100 μm).
(B) Immunofluorescence microscopy using a DSTYK C-terminal antibody (1:500, Santa Cruz Biotechnology cat# sc-374487, RRID: AB_10988978) in normal skin (top) reveals bright pan-epidermal cytoplasmic staining with focal accentuation in basal epidermal melanocytes and dermal fibroblasts. In affected individual (IV-5) skin (middle) there is markedly reduced labeling, with an absence of staining in the negative control (bottom).
(C) Transmission electron micrograph of a melanocyte (affected individual IV-5) shows prominent mitochondria and abnormal cytoplasmic vacuoles (asterisk) (scale bar represents 2 μm).
(D) Transmission electron micrograph of a keratinocyte (affected individual IV-5) shows prominent swollen mitochondria with abnormal cristae (asterisks) (scale bar represents 2 μm).

To further explore the potential role for DSTYK in regulating cell death, primary fibroblasts and keratinocytes from this affected individual were isolated for further analysis, with the keratinocytes immortalized at passage 1. We also generated *Dstyk* siRNA knockdown mouse fibroblasts, keratinocytes, and melanocytes to determine whether siRNA-depleted cells and cells from affected individuals exhibited similar phenotypes. We first assessed whether loss of DSTYK resulted in increased cell death. Cells were exposed to a UV illuminator for 2 min and fixed after 9 hr and apoptosis levels were determined by analysis of total cell number as a readout for cell death. For all cell types, both *Dstyk* knockdown and mutant cells exhibited increased cell death 9 hr after exposure to UV as shown by loss of cell attachment (Figures 3A–3E). There were no differences in cell death between *Dstyk*-depleted and control cells under basal conditions (data not shown). As alternative readouts for UV-induced apoptosis, cleaved caspase-3 staining was also assessed and apoptotic markers were analyzed by FACS analysis after UV treatment. A significant increase in cells positive for cleaved caspase-3 staining was observed in DSTYK-depleted keratinocytes and melanocytes after 9 hr of UV exposure (Figures S5A–S5C); FACS analysis also revealed an increase in Annexin V and 7-AAD labeling in mutant fibroblasts compared to controls, reflecting an increase in both early and late apoptotic markers (Figure S5D), which confirmed the increased susceptibility to apoptotic signaling due to the loss of DSTYK protein. To assess whether loss of DSTYK altered mitochondrial architecture, we stained live knockdown and mutant cells with MitoTracker Red followed by fixation and analysis by confocal microscopy. All cell types showed dispersed and enlarged mitochondrial organization in response to UV, but no marked changes in this response were observed in *Dstyk* knockdown or mutant cells compared to control cells (Figures S6A–S6C and data not shown). DSTYK has previously been shown to be a positive regulator of extracellular signal-regulated kinase (ERK) phosphorylation downstream of FGF stimulation in HEK293T cells.[18] We therefore determined whether cells from affected individuals showed loss of pERK activity upon FGF stimulation. Biochemical analysis demonstrated that primary mutant keratinocytes showed significantly reduced pERK activation in response to FGF stimulation compared to control cells (Figures S7A and S7B), confirming previous observations on the role of DSTYK in regulating FGF signaling.

Our study indicates that the molecular basis of SPG23, at least in three pedigrees, involves a large 3′ deletion in *DSTYK*, and thus two specific disease entities, SPG23 and

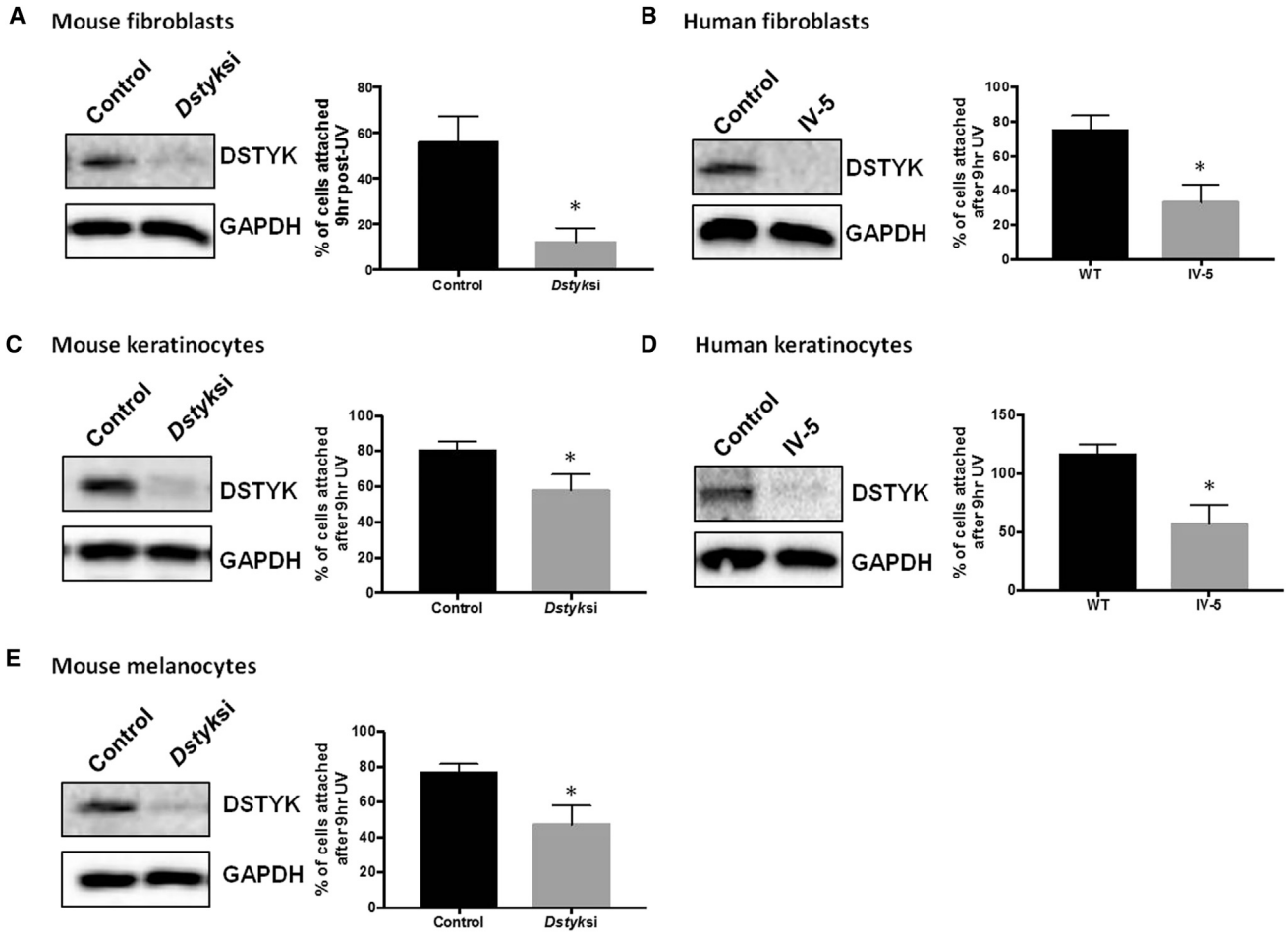

Figure 3. Increased Sensitivity to Apoptosis in DSTYK-Null Cells

(A) Western blots of DSTYK protein levels in mouse NIH 3T3 fibroblasts transfected with non-targeting siRNA (control) or siRNA pool specifically targeted to *Dstyk* (*Dstyk*si). Graph shows percentage of total starting cells attached 9 hr after UV illumination. Values are means ± standard error of the mean (SEM). Representative of three independent experiments. *$p < 0.05$.

(B) Western blots of DSTYK protein levels in human fibroblasts isolated from healthy donors (control) or affected individual (IV-5). Graph shows percentage of total starting cells attached 9 hr after UV illumination. Values are means ± SEM. Representative of three independent experiments. *$p < 0.05$.

(C) Western blots of DSTYK protein levels in mouse keratinocytes transfected with non-targeting siRNA (control) or siRNA pool specifically targeted to *Dstyk* (*Dstyk*si). Graph shows percentage of total starting cells attached 9 hr after UV illumination. Values are means ± SEM. Representative of three independent experiments. *$p < 0.05$.

(D) Western blots of DSTYK protein levels in human keratinocytes isolated from healthy donors (control) or affected individual (IV-5). Graph shows percentage of total starting cells attached 9 hr after UV illumination. Values are means ± SEM. Representative of three independent experiments. *$p < 0.05$.

(E) Western blots of DSTYK protein levels in mouse melanocytes transfected with non-targeting siRNA (control) or siRNA pool specifically targeted to *Dstyk* (*Dstyk*si). Graph shows percentage of total starting cells attached 9 hr after UV illumination. Values are means ± SEM. Representative of three independent experiments. *$p < 0.05$.

CAKUT1, harbor mutations in the same gene. Aside from the different mode of inheritance, the heterozygous mutations in CAKUT1 have been mostly upstream of the kinase domain, with the exception of one missense mutation in exon 12.[18] In contrast, the intragenic deletion we identified occurs near the C terminus and appears to lead to reduction of protein levels. Nevertheless, a minor overlap in phenotype occurs—with the SPG23 proband in our study also having a structural renal anomaly, and some neurologic features being described in CAKUT1. Overall, the lack of urinary tract abnormalities in heterozygotes and some homozygotes in the three SPG23 pedigrees presented in our study indicates that this novel deletion has a distinct functional impact. Morpholino knockdown of *dstyk* in zebrafish was shown to result in a wide spectrum of defects including growth retardation, abnormal tail morphogenesis, loss of heartbeat, cloacal malformations, and abnormalities in jaw development.[18] *Dstyk* kinase domain-knockout mice showed impaired learning and memory capabilities but had no significant morphological defects.[19] The apparent discrepancy between the features seen in mutant mice with CAKUT1 and SPG23 cases may be due to the fact that full-length DSTYK was not ablated in these mice and a truncated protein may still have

been present.[19] Moreover, our data suggest that DSTYK acts to suppress apoptosis in response to UV-induced stress, the response to which remains unknown in animal models of DSTYK dysfunction.

Our data suggest that loss of DSTYK in fibroblasts, keratinocytes, and melanocytes leads to increased susceptibility to apoptosis (quantified by cell number, cleaved caspase-3 staining, and FACS analysis). Various modalities of cell death can occur, including necrosis, necroptosis, and pyroptosis,[20] and mitochondrial swelling has also been associated with non-apoptotic forms of programmed cell death.[21] DSTYK has previously been proposed to be a positive regulator of both caspase-dependent and -independent cell death pathways.[14] However, this was shown to occur only after overexpression of DSTYK in HEK293 cells and in the absence of external stress stimuli. Our data show that in the context of skin, DSTYK plays a predominant role in suppressing caspase-dependent apoptosis in response to UV stress in a range of dermal cell types. Future studies will focus on understanding the mechanisms by which DSTYK contributes to apoptosis protection.

One pertinent clinical feature in the skin in individuals with SPG23 is loss of skin pigment: some of this pathology may reflect post-inflammatory hypopigmentation but certain lesions show complete depigmentation in keeping with vitiligo, a common complex disorder associated with autoimmune destruction of melanocytes in skin and hair. Other cases of vitiligo may show familial clustering although inheritance is non-Mendelian and multi-factorial.[22] To date, approximately 40 loci with convincing or strongly suggestive evidence for a role in vitiligo susceptibility have been identified,[23] although there has been no association with *DSTYK* or its locus on 1q32.1, indicating that DSTYK may not be involved in common complex versions of this condition. The vitiligo in our cases likely reflects localized cell killing of melanocytes, although how the deletion in *DSTYK* preferentially leads to melanocyte loss is uncertain, particularly given the presence of abnormal vacuoles and swollen mitochondria in several skin cell types, including melanocytes, keratinocytes, and fibroblasts. Both melanocytes and Schwann cells are derived from the neural crest, and these two distinct cell types have been proposed to originate from a common post-neural crest progenitor, namely the Schwann cell precursor.[24] The motor and pigmentary symptoms in individuals with SPG23 may be a manifestation of increased vulnerability of Schwann cell precursors to cell death, but further studies in appropriate model systems are needed to dissect the underlying pathomechanisms of this unique disorder.

In summary, we have identified a large intragenic deletion in *DSTYK* as the molecular basis for three families with SPG23, an autosomal-recessive disorder characterized by spastic paraparesis and dyspigmentation. Our data in skin tissue also indicate the clinical consequences of abnormal cell death, highlighting findings of potential relevance to other more common disease processes in the skin, such as vitiligo and other dyspigmentary dermatoses.

Supplemental Data

Supplemental Data include eight figures and five tables and can be found with this article online at http://dx.doi.org/10.1016/j.ajhg.2017.01.014.

Acknowledgments

The Centre for Dermatology and Genetic Medicine is supported by a Wellcome Trust Strategic Award (reference 098439/Z/12/Z). The work was supported by the MRC (MR/M018512/1) and the UK National Institute for Health Research (NIHR) comprehensive Biomedical Research Centre (BRC) award to Guy's and St. Thomas' NHS Foundation Trust, in partnership with the King's College London and King's College Hospital NHS Foundation Trust. This study was also supported by UK Medical Research Council Project Grant (MR/M00046X/1) and Action Research grant SP3706 as well as medical student grants from the Jean Shanks Foundation and the British Association of Dermatologists. We thank Akemi Ishida-Yamamoto (Asahikawa, Japan) for help with transmission electron microscopy analysis.

Received: September 11, 2016
Accepted: January 5, 2017
Published: February 2, 2017

Web Resources

BLAST, http://blast.ncbi.nlm.nih.gov/Blast.cgi
CNVD, http://202.97.205.78/CNVD/index.jsp
Database of Genomic Variants (DGV), http://dgv.tcag.ca/dgv/app/home
DECIPHER, http://decipher.sanger.ac.uk/
Ensembl Genome Browser, http://www.ensembl.org/index.html
OMIM, http://www.omim.org/
Primer3, http://bioinfo.ut.ee/primer3
PubMed, http://www.ncbi.nlm.nih.gov/PubMed/
RefSeq, http://www.ncbi.nlm.nih.gov/RefSeq

References

1. Hensiek, A., Kirker, S., and Reid, E. (2015). Diagnosis, investigation and management of hereditary spastic paraplegias in the era of next-generation sequencing. J. Neurol. *262*, 1601–1612.
2. Abdallat, A., Davis, S.M., Farrage, J., and McDonald, W.I. (1980). Disordered pigmentation, spastic paraparesis and peripheral neuropathy in three siblings: a new neurocutaneous syndrome. J. Neurol. Neurosurg. Psychiatry *43*, 962–966.
3. Lison, M., Kornbrut, B., Feinstein, A., Hiss, Y., Boichis, H., and Goodman, R.M. (1981). Progressive spastic paraparesis, vitiligo, premature graying, and distinct facial appearance: a new genetic syndrome in 3 sibs. Am. J. Med. Genet. *9*, 351–357.
4. Mukamel, M., Weitz, R., Metzker, A., and Varsano, I. (1985). Spastic paraparesis, mental retardation, and cutaneous pigmentation disorder. A new syndrome. Am. J. Dis. Child. *139*, 1090–1092.

5. Bamforth, J.S. (2003). Vitiligo-spasticity syndrome: new case. Clin. Dysmorphol. *12*, 137–139.
6. Mandal, S., and Bid, D. (2009). Vitiligo with spastic paraparesis: A rare neurocutaneous syndrome. J. Pediatr. Neurol. *7*, 329–331.
7. Blumen, S.C., Bevan, S., Abu-Mouch, S., Negus, D., Kahana, M., Inzelberg, R., Mazarib, A., Mahamid, A., Carasso, R.L., Slor, H., et al. (2003). A locus for complicated hereditary spastic paraplegia maps to chromosome 1q24-q32. Ann. Neurol. *54*, 796–803.
8. Plagnol, V., Curtis, J., Epstein, M., Mok, K.Y., Stebbings, E., Grigoriadou, S., Wood, N.W., Hambleton, S., Burns, S.O., Thrasher, A.J., et al. (2012). A robust model for read count data in exome sequencing experiments and implications for copy number variant calling. Bioinformatics *28*, 2747–2754.
9. Firth, H.V., Richards, S.M., Bevan, A.P., Clayton, S., Corpas, M., Rajan, D., Van Vooren, S., Moreau, Y., Pettett, R.M., and Carter, N.P. (2009). DECIPHER: Database of Chromosomal Imbalance and Phenotype in Humans Using Ensembl Resources. Am. J. Hum. Genet. *84*, 524–533.
10. MacDonald, J.R., Ziman, R., Yuen, R.K., Feuk, L., and Scherer, S.W. (2014). The Database of Genomic Variants: a curated collection of structural variation in the human genome. Nucleic Acids Res. *42*, D986–D992.
11. Qiu, F., Xu, Y., Li, K., Li, Z., Liu, Y., DuanMu, H., Zhang, S., Li, Z., Chang, Z., Zhou, Y., et al. (2012). CNVD: text mining-based copy number variation in disease database. Hum. Mutat. *33*, E2375–E2381.
12. Chen, J.M., Chuzhanova, N., Stenson, P.D., Férec, C., and Cooper, D.N. (2005). Intrachromosomal serial replication slippage in trans gives rise to diverse genomic rearrangements involving inversions. Hum. Mutat. *26*, 362–373.
13. Sheen, C.R., Jewell, U.R., Morris, C.M., Brennan, S.O., Férec, C., George, P.M., Smith, M.P., and Chen, J.M. (2007). Double complex mutations involving F8 and FUNDC2 caused by distinct break-induced replication. Hum. Mutat. *28*, 1198–1206.
14. Zha, J., Zhou, Q., Xu, L.G., Chen, D., Li, L., Zhai, Z., and Shu, H.B. (2004). RIP5 is a RIP-homologous inducer of cell death. Biochem. Biophys. Res. Commun. *319*, 298–303.
15. Meylan, E., and Tschopp, J. (2005). The RIP kinases: crucial integrators of cellular stress. Trends Biochem. Sci. *30*, 151–159.
16. Peng, J., Dong, W., Chen, Y., Mo, R., Cheng, J.F., Hui, C.C., Mohandas, N., and Huang, C.H. (2006). Dusty protein kinases: primary structure, gene evolution, tissue specific expression and unique features of the catalytic domain. Biochim. Biophys. Acta *1759*, 562–572.
17. Diehn, M., Sherlock, G., Binkley, G., Jin, H., Matese, J.C., Hernandez-Boussard, T., Rees, C.A., Cherry, J.M., Botstein, D., Brown, P.O., and Alizadeh, A.A. (2003). SOURCE: a unified genomic resource of functional annotations, ontologies, and gene expression data. Nucleic Acids Res. *31*, 219–223.
18. Sanna-Cherchi, S., Sampogna, R.V., Papeta, N., Burgess, K.E., Nees, S.N., Perry, B.J., Choi, M., Bodria, M., Liu, Y., Weng, P.L., et al. (2013). Mutations in DSTYK and dominant urinary tract malformations. N. Engl. J. Med. *369*, 621–629.
19. Li, K., Liu, J.W., Zhu, Z.C., Wang, H.T., Zu, Y., Liu, Y.J., Yang, Y.H., Xiong, Z.Q., Shen, X., Chen, R., et al. (2014). DSTYK kinase domain ablation impaired the mice capabilities of learning and memory in water maze test. Int. J. Clin. Exp. Pathol. *7*, 6486–6492.
20. Kroemer, G., Galluzzi, L., Vandenabeele, P., Abrams, J., Alnemri, E.S., Baehrecke, E.H., Blagosklonny, M.V., El-Deiry, W.S., Golstein, P., Green, D.R., et al.; Nomenclature Committee on Cell Death 2009 (2009). Classification of cell death: recommendations of the Nomenclature Committee on Cell Death 2009. Cell Death Differ. *16*, 3–11.
21. Sperandio, S., de Belle, I., and Bredesen, D.E. (2000). An alternative, nonapoptotic form of programmed cell death. Proc. Natl. Acad. Sci. USA *97*, 14376–14381.
22. Spritz, R.A. (2013). Modern vitiligo genetics sheds new light on an ancient disease. J. Dermatol. *40*, 310–318.
23. Shen, C., Gao, J., Sheng, Y., Dou, J., Zhou, F., Zheng, X., Ko, R., Tang, X., Zhu, C., Yin, X., et al. (2016). Genetic susceptibility to vitiligo: GWAS approaches for identifying vitiligo susceptibility genes and loci. Front. Genet. *7*, 3.
24. Adameyko, I., Lallemend, F., Aquino, J.B., Pereira, J.A., Topilko, P., Müller, T., Fritz, N., Beljajeva, A., Mochii, M., Liste, I., et al. (2009). Schwann cell precursors from nerve innervation are a cellular origin of melanocytes in skin. Cell *139*, 366–379.